J Polym Res (2011) 18:2341–2350
DOI 10.1007/s10965-011-9647-x

ORIGINAL PAPER

High strength poly(acrylamide)-clay hydrogels

**Ekmel Helvacıoğlu · Volkan Aydın · Turgut Nugay ·
Nihan Nugay · Bilge G. Uluocak · Sinan Şen**

Received: 31 December 2010 / Accepted: 21 June 2011 / Published online: 1 July 2011

Abstract A series of polyacrylamide nanocomposite hydrogels were synthesized by *in situ* free radical polymerization of acrylamide (AAm) with ethylene glycol dimethacrylate (EGDMA) as a crosslinker in the presence of sodium montmorillonite (NaMMT) and organically modified montmorillonite (OrgMMT) clays. Modification of MMT was carried out with a quaternary salt of coco amine as intercalant having a styryl group whose contribution to both polymerization and crosslinking reactions via its reactive double bond was confirmed by solid state NMR. Exfoliation success was checked with X-ray diffraction (XRD) and atomic force microscopy (AFM) techniques whereas mechanical performance was followed with uniaxial compression experiment. It has been found that exfoliated PAAm nanocomposites having 0.5% OrgMMT had both the maximum equilibrium swelling in water and compression strength as well as improved thermal stability due to the special and beneficial morphology observed via scanning electron microscopy (SEM).

Keywords Hydrogels · Polyacrylamide · Nanocomposite hydrogel · High strength hydrogels

Introduction

In recent years, polymeric hydrogels have attracted a great deal of attention because of characteristic properties such as swell ability in water, hydrophilicity, and biocompatibility. The ability to absorb and to store much water and water solutions make hydrogels as unique materials for a variety of applications. They have found widespread applications in biomedicine, food industry and water purification and separation process [1–4]. Among them, acrylamide based hydrogels are quite important due to their use in many sorbent applications and like any other hydrogels they are usually produced by free radical polymerization in the presence of crosslinker. On the other hand, their soft and very brittle nature making them mechanically weak materials in swollen state limit their application areas.

In order to overcome this drawback, studies have been focused on redesigning the hydrogels with high mechanical performances via organic nanoparticle addition [5], interpenetrating network formation [6–9], hydrophilic reactive microgel formation [10] as well as inorganic nanoparticle addition [11]. Among them, nanoscale dispersion of clays in polymer networks were most extensively studied ones due to their inherent good absorbance, high mechanical strength, toughness and high chemical resistance properties. Several kinds of inorganic clay particles including Na-montmorillonite, attapulgite and Laponite–synthetic hectorite, have been introduced to PAAm gel systems with or without the additional use of chemical crosslinkers. It is very well known that the extent of crosslinking is usually the factor in determining both swelling capacity and mechanical strength. Due to its inherent multifunctional crosslinker action, laponite was studied extensively especially in terms of its pH sensibility, swelling and elastic [11], dye absorption properties [12], rheological and light scattering properties [13] and tensibility [14]. Okay et al. [11] reported that although modulus of elasticity

E. Helvacıoğlu · V. Aydın · T. Nugay · N. Nugay
Department of Chemistry and The Polymer Research Center,
Bogazici University, Bebek,
34342 İstanbul, Turkey

B. G. Uluocak
Advanced Technologies Research and Development Center,
Bogazici University, Bebek,
34342 İstanbul, Turkey

S. Şen (✉)
Department of Polymer Engineering, Yalova University,
77100 Yalova, Turkey
e-mail: sinans@yalova.edu.tr

increases with laponite content, only 1–4 kPa values were found to be attainable with loading degree which must be higher than 6%.

On the other hand, polyacrylamide-bentonite based hydrogels found special interest in literature especially in their crosslinker free preperation of hydrogels with super-absorption capacity as well as their rheological characterization [15]. Moreover some attempts have been made to prepare novel nanocomposite type of hydrogels by crosslinking the partially hydrolized polyacrylamide-montmorillonite (Na-MMT) clay aqueous solutions with chromium as crosslinker, in which the clay layers with high aspect ratio are exfoliated through the polymer matrix and acting as multifunctional crosslinker [16]. The effects of the composition, such as clay content, crosslinker concentration and also water salinity upon the gelation rate, gel strength as well as rate of syneresis have been investigated. The nanocomposite gels showed increased elasticity and extensibility at low crosslinker concentration compared with the similar but unfilled gel, which makes the nanocomposite gels suitable as an in-depth profile modifier, and also as an oil displacing agent in the heterogeneous oil reservoir in chemical enhanced oil recovery. On the other hand, a systematic study on mechanical performance of these types of nanocomposite hydrogels seems to be needed.

In this study, polyacrylamide-MMT nanocomposite hydrogels were prepared by *in-situ* free-radical polymerization in aqueous clay suspensions in the presence of crosslinker, ethylene glycol dimethacrylate. The MMT clay was rendered organophilic with a quaternary salt of coco amine having a styrly part as the reactive group for both co-crosslinking and polymerization reactions. The cocoamine salt is expected to intercalate between the clay layers via ionic interactions and participate in both polymerization and crosslinking reactions via its reactive double bond. This may lead to exfoliated nanocomposite structure via existence of nanolayer connected intercelant-co-crosslinker serving to crosslinking process and leading to strong and extensible multifunctional crosslink domains between the nanodispersed layers which then may be resulting in an enhanced mechanical strength in the hydrogel. The gel strength and water absorbency as well as thermal stability of the resultant nanocomposite hydrogels interms of morphologyl are all discussed as a function of nature of functional intercalant, crosslinking degree and degree of clay loading.

Experimental

Materials

Acrylamide (AAm), the initiator, ammonium persulfate (APS) and the activator, sodium metabisulfite (SMBS) were bought from Merck (Darmstad, Germany) and used without furher purification. The crosslinker, ethylene glycol dimethacrylate (EGDMA) was supplied by Aldrich Chemicals (Milwaukee, US).

The clay, sodium montmorillonite (NaMMT) was kindly donated by Süd Chemie (Nanofil 1080, cationic [Na^+] exchange capacity of 100 meq/100 g). The chemical structure of the modifier, quaternary cocoamine salt, having a vinyl group and a tail with up to 18 carbons composed of *ca* 6% C8, *ca* 4% C10, *ca* 48% C12, *ca* 21% C14, *ca* 11% C16 and *ca* 10% C18 alkyl chains [17] is depicted in Fig. 1.

Modification of NaMMT with quaternary salt of coco amine

NaMMT (2 g) was dispersed in 200 mL of deionized water at 80 °C and a separate solution of 1 g of quaternary coco amine salt, modifier, in 100 mL of deionized water was slowly added to the clay solution and mixed vigorously, while keeping the temperature of the solution at 80 °C. After mixing, the total volume is brought up to 400 mL and stirred for 1 h. The organically modified MMT (OrgMMT) was recovered by filtering the solution, followed by repeated washings of the filter cake with deionized water to remove excess ions. The final product was dried at 50 °C in a vacuum oven for 48 h.

Preparation of polyacrylamide nanocomposite hydrogels

The hydrogels were prepared by the *in situ* free radical polymerization of AAm in the presence of the water-swollen inorganic clay with using the organic crosslinker, EGDMA. An aqueous solution consisting of deionized water (5 mL), various amounts of NaMMT and OrgMMT clays (0.1%, 0.5% and 1% by weight of monomer) and AAm (5 g) was prepared. Then the crosslinker, EGDMA (1 mol% with respect to monomer) was added to this solution. After mixing a few minutes and introducing nitrogen gas, the catalyst (0.1 mol%, based on monomer) and subsequently the initiator (APS, 0.3 mol%, based on monomer) were added to this mixture with stirring. The hydrogels were synthesized in airtight glass tubes**.** Then, the polymerization was conducted in a water bath at 30 °C for 48 h.

The resultant nanocomposite hydrogels are referred as PAAm-XNaM and PAAm-XOrgM, where X represents the

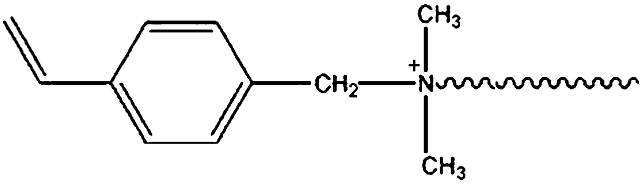

Fig. 1 Molecular structure of quaternary coco amine

clay loading percent in the form of NaMMT and Organophilic MMT, respectively.

Characterization

X-ray diffraction (XRD) measurements of NaMMT and OrgMMT clays as well as dried hydrogels were conducted on a Rigaku D/Max 2200 Ultimat diffractometer (Rigaku, Tokyo, Japan) with CuK$_\alpha$ radiation (λ=1.54°A), operating at 40 kV and 40 mA with a scanning rate of 2°/min.

Morphology of the nanocomposite hydrogels were investigated by XRD, atomic force microscopy (AFM) and scanning electron microscopy (SEM) measuements. AFM analysis was performed using a Universal Scanning Probe Microscope (USPM) (Ambios Technology, Santa Cruz, CA). Phase-mode imaging was performed using a silicon nitride cantilever probe (NSC16) with a spring constant of 25–60 N/m. Phase images were obtained in tapping mode in which the cantilever was oscillated at its resonance frequency of 170 kHz. Samples were prepared for AFM investigation by spin-coating the aqueous monomer-clay solution together with crosslinker, catalyst and initiator onto pre-cleaned glass-slide and were spin-coated at 500 rpm. The sample was cured at 30 °C for 48 h. SEM analyses of freeze-dried hydrogels were carried out by using ESEM-FEG/EDAX Philips XL-30 (Philips, Eindhoven, The Netherlands).

Thermogravimetric analysis (TGA) was performed on TGA-Q50 instrument (TA Instruments, New Castle, DE, USA) under nitrogen flow with a heating rate of 10 °C/min.

Swelling behaviour of the hydrogels was followed by gravimetric measurements. The freeze-dried polymeric samples were weighed and immersed in deionized water and taken out at regular intervals of time to measure change in weight. Water uptake with respect to time was obtained by periodically removing the samples from water, quickly drying, and reweighing. The measurements were conducted at 25 °C in a water bath. The percent swelling (water uptake) was calculated with the following equation:

$$S\ \% = \frac{m_t - m_0}{m_0} \ *100 \qquad (1)$$

where m_t is the mass of the swollen gel at time t and m_o is the mass of the dry gel.

The mechanical strengths of the hydrogels were measured by performing uniaxial compression experiment with Devotrans DVT-G 21 Model tester (Istanbul, Turkey) with a compression rate of 2 mm/min. All the mechanical measurements were performed on equilibrium water-swollen gels, which are cut into cylindrical samples of about 20 mm in length, at room temperature. The measurements were conducted until the samples fracture. The compression force acting on the gel *versus* deformation as well as elastic modulus were obtained from the original output of instrument.

^{1}H NMR spectrum of the quaternary coco amine salt was recorded with a 400 MHz Varian Mercury-VX NMR spectrometer (Varian Associates, Palo, Alta, CA). Solid-State ^{1}H NMR spectrum of the PAAm-0.5OrgM nanocomposite hydrogel was recorded with a Bruker DSX-300 spectrometer.

Results and discussion

Clay modification

Modification of the MMT clay was followed with X-ray diffraction analysis. XRD analysis gave the values of the interlayer spacing or *d*-spacing of the NaMMT and OrgMMT which were obtained from the peak position of the d_{001} reflection in the diffraction patterns (Fig. 2). A 2θ angle of 7.28° and basal spacing of 12.13 A° was found for NaMMT clay. It can be seen from the Fig. 2 that diffraction angle of OrgMMT was found to be lower (3.5°) and its interlayer spacing was found to be 21 A°. Thus, a decrease in the diffraction angle and increase in interlayer distance indicates that intercalation of quaternary coco amine salt into MMT clay layers through the ion-exchange reaction was successful, resulting in an organophilic clay. The existence of quaternary coco amine salt in the MMT structure was also confirmed by TGA. Figure 3 shows the TGA scans of NaMMT and OrgMMT clays. It is clear from the Fig. 3 that OrgMMT shows a lower decomposition onset temperature as well as higher degradation dependent weight loss compared to pure NaMMT. Pure MMT has only 10% total weight loss indicating water removal. After the intercalation, this amount reaches almost 35% at higher

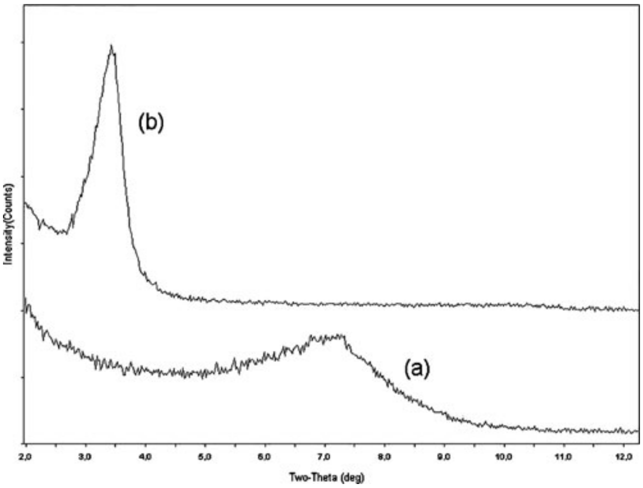

Fig. 2 X-ray diffractograms of (**a**) NaMMT and (**b**) OrgMMT

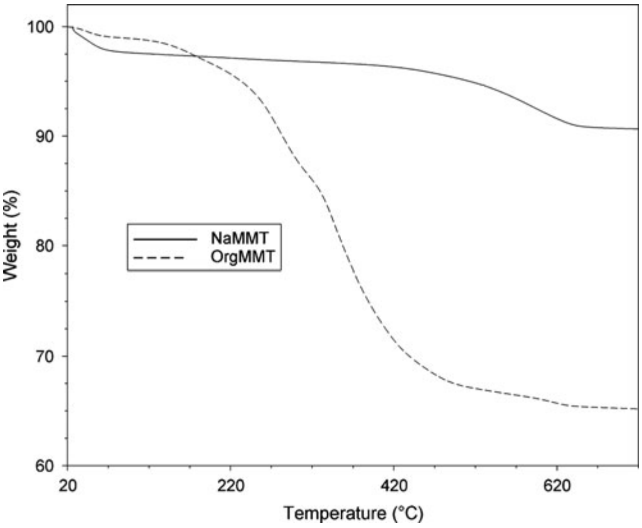

Fig. 3 TGA thermograms of NaMMT and OrgMMT clays

temperatures, resulting from the degradation of intercalated and edge/surface attached coco amine salt. This result can be accepted as an indication of the successful modification of the MMT clay.

Morphology and properties nanocomposite hydrogels

Degree of dispersion of both unmodified and modified montmorillonite in polyacrylamide nanocomposite hydrogels was also determined by XRD analyses. Figure 4 shows X-ray diffractograms of PAAm-NaM samples. As it can be seen from the figure, there is no noticeable MMT clay peak (d_{001} reflection) appearing in their diffraction patterns, leading to exfoliation. This result may be ascribed to the homogeneous dispersion of the clays, which does not present any more ordering, or a too large spacing between the layers exceeding 8 nm in the case of exfoliated structure [18].

Figure 5 shows the XRD curves of PAAm-OrgM nanocomposite hydrogels. It can be seen that the nanocomposite, PAAm-1OrgM exhibited a peak with a *d*-spacing value of 15.74 A° in the relevant angle region representing the diffraction from the (001) crystal surface of the silica layers as an indication of intercalated nanocomposite structure. This may result from some amount of multilayer tactoids of OrgMMT clay and polymer chains. Moreover, the relatively smaller and broader nature of this peak could be accepted as proof of the existence of a partially exfoliated or intercalated structure [18]. On the other hand, PAAm-0.1OrgM and PAAm-0.5OrgM exhibited complete exfoliated structure with the absence of any d_{001} reflection in the XRD region. This may be possibly due to good swelling of OrgMMT clay and homogeneous as well as fine dispersion of it in the matrix.

Figure 6 shows AFM phase image of nanocomposite hydrogel, PAAm-0.5OrgM. In the tapping mode AFM, the phase contrast in the image is caused by repulsive probe tip-sample interactions with the nanosilica, resulting in a positive phase and bright areas or features corresponding to nano-sized silica phase [19, 20]. The nano-scale dispersion was also easily observed in AFM images. Exfoliation is quite clear and the nano-sized clays with an average thickness of 32 nm are separated from each other as a further confirmation of the XRD peak disappearance mentioned above.

The swelling behavior of the PAAm hydrogels prepared with different amounts of NaMMT and OrgMMT clays are shown in Fig. 7 and Fig. 8.

Both figures show that swelling increases with time up to certain level and then levels off as an indication of equilibrium between swelling and deswelling. These equilibrium swelling values are all given in Table 1. Both Table 1 and Fig. 7 indicate that the maximum attainable swelling in neat PAAm network having crosslinker is 577%

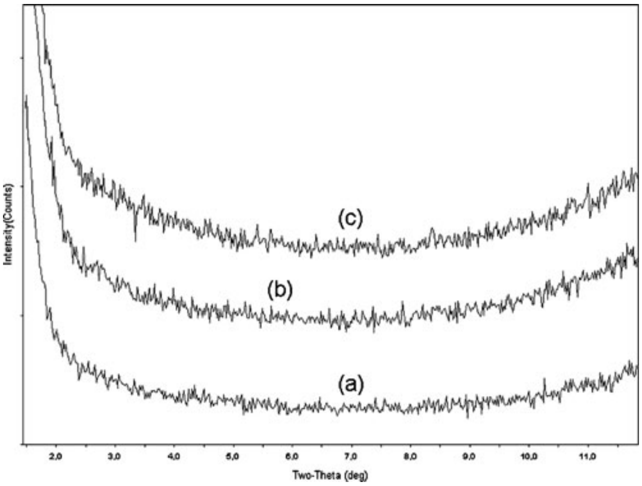

Fig. 4 X-ray diffraction curves of (**a**) PAAm-0.1NaM, (**b**) PAAm-0.5NaM and (**c**) PAAm-1NaM

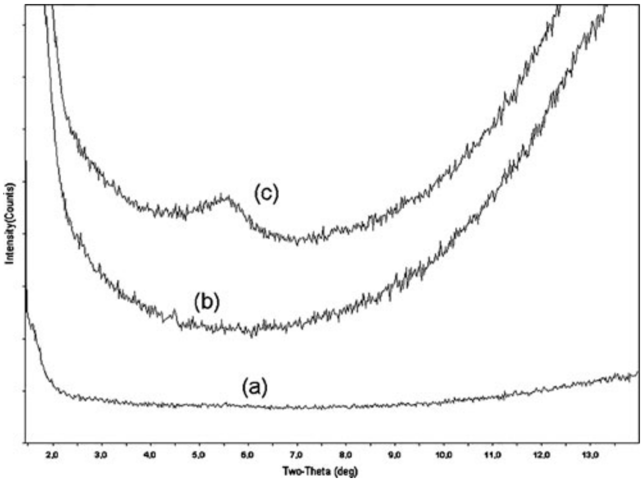

Fig. 5 X-ray diffraction curves of (**a**) PAAm-0.1OrgM, (**b**) PAAm-0.5OrgM and (**c**) PAAm-1OrgM

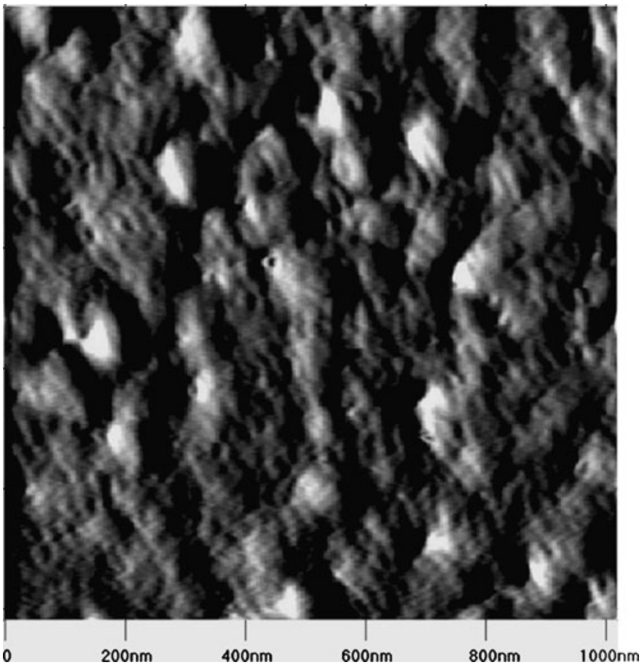

Fig. 6 AFM phase image of PAAm-0.5OrgM

whereas the values for most nanocomposite hydrogels are higher. It is very well known that the conventional hydrogels prepared using organic cross-linkers have serious disadvantages arising from random arrangements of large numbers of cross-links which is leading to insufficient swelling/deswelling properties [21]. It is also quite clear from the figure that the higher values of swelling for the nanocomposite hydrogels belong to the ones having 0.1% and 0.5% NaMMT clay most probably due to the increased hydrophilic character with hydrophilic clay addition as well as nanolayer guided well dispersion of crosslinking. Interestingly, in higher loaded hydrogel, swelling value decreases abruptly even below the neat hydrogel. This result may be attributed to possible disturbance of the network structures. On the other hand, increased swelling of PAAm-1NaM hydrogel up to 150 min at a much higher rate compared to other systems may result from the increased hydrophilicity via filler content but then levelling off at 447%, probably, due to the insufficient accommodation of water in the pores.

Insertion of OrgMMT clay into hydrogel at 0.5% loading, on the other hand, causes to a peak in equilibrium swelling values up to 700% (Fig. 8). But, this extreme swelling decreases to a lower values at 0.1 and 1% loadings. The lower values of water-uptake in these loadings may be ascribed to increase in hydrophobic group in the clay but still having a value higher than that of PAAm-1NaM which may be attributed to finer dispersion-guided larger surface area of OrgMMT clay than NaMMT. Moreover, organophilic clay may behave as additional junctions with the help of reactive double bond in the intercalant. So, the amount of crosslink increases with increasing of OrgMMT up to 1% which might be the reason for decreasing of swelling value with increasing amount of OrgMMT clay. Another effective mechanism would be probably the existence of the less amount of expanded clay incorporated as indicated by the XRD results. It seemed that when the amount of OrgMMT clay was around 0.5%, the hydrogel can be tuned for serving as a good water absorber, most probably, due to homogeneous and fine distribution of pre-expanded clay layers in the polymer matrix and formation of an additional extended subnetwork between AAm and the clay via reactive double bond on

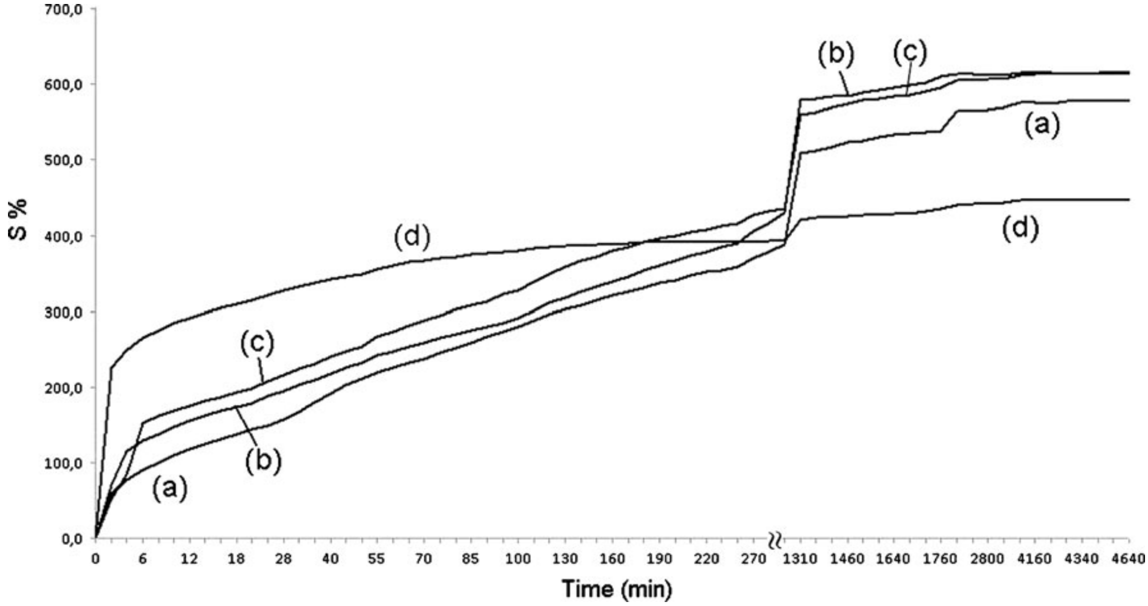

Fig. 7 Percentage swelling of (**a**) PAAm, (**b**) PAAm-0.1NaM, (**c**) PAAm-0.5NaM and (**d**) PAAm-1NaM hydrogels in water

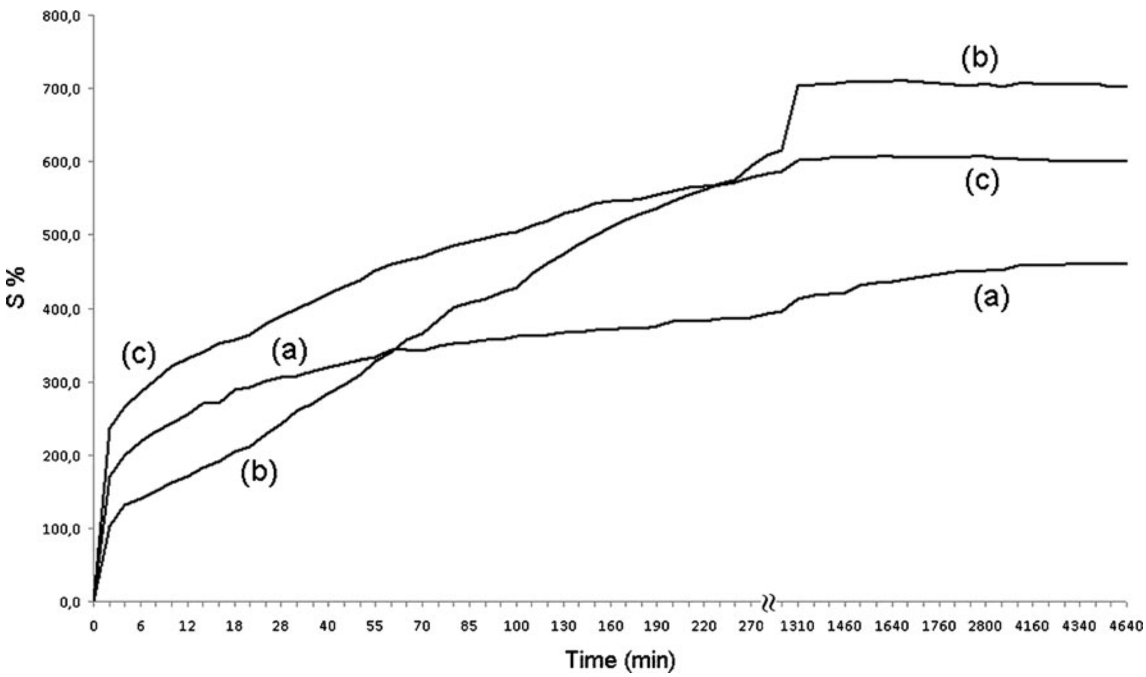

Fig. 8 Percentage swelling of (**a**) PAAm-0.1OrgM, (**b**) PAAm-0.5OrgM and (**c**) PAAm-1OrgM hydrogels in water

intercalant. Contribution of these reactive double bonds to crosslinking/polymerization was also confirmed with NMR analyses (Fig. 9). The ^{1}H-NMR spectrum of quaternary coco amine (Fig. 9a) showed a triplet between 5.3–5.4 ppm and a doublet at 5.8 ppm which belong to the vinyl group protons in the quaternary coco amine salt. After nanocomposite formation disappearance of these peaks (Fig. 9b) can be accepted as clear indication for the participation of the double bond to polymerization/crosslinking reaction.

The mechanical properties of PAAm nanocomposite gels were investigated in terms of compression strength. The compression force-deformation data of the gels are shown in Fig. 10 and Fig. 11 as well as in Table 2.

Gel strength of the nanocomposites was found to be greater than that of neat PAAm gel having only organic crosslinker inside. The elastic modulus as well as toughness (area under stress - strain curve) of the hydrogels increase with increasing OrgMMT clay concentration up to 0.5%. It is well known that due to heterogeneously distributed crosslink points in the matrix, the conventional chemically crosslinked hydrogels (OR gels) are quite weaker than the nanocomposite hydrogels in terms of mechanical, optical, swelling/deswelling properties [22]. Although, in the literature, it has been reported that the use of both clay as reinforcer and N,N-methylenebisacrylamide as crosslinker resulted in poor mechanical properties which are similar to those of conventional OR gels [23–25], having extraordinary high mechanical strength for the hydrogels in our study is remarkable. The construction of these high strength nanocomposite hydrogels is believed to be achieved by incorporation of organophilic nano-platelets instead of an hydrophilic clay into the crosslinked network with contribution to crosslinking via their double bonds together with

Table 1 Equilibrium percentage swelling data for hydrogels

Hydrogels	Equilibrium Percentage Swelling (S_{eq}%)
Neat PAAm	577
PAAm-0.1NaM	614
PAAm-0.5NaM	613
PAAm-1NaM	447
PAAm-0.1OrgM	459
PAAm-0.5OrgM	705
PAAm-1OrgM	601

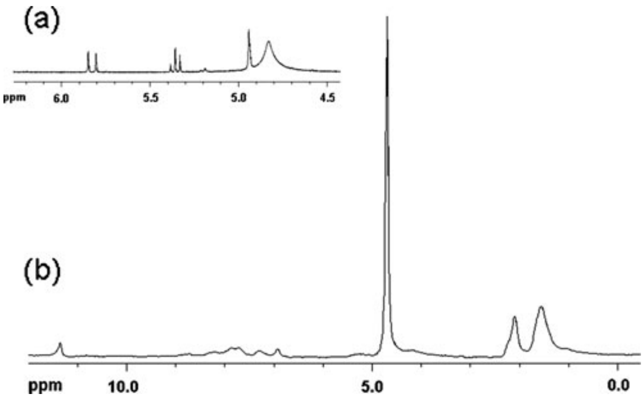

Fig. 9 ^{1}H NMR spectra of (**a**) quaternary coco amine and (**b**) PAAm-0.5OrgM

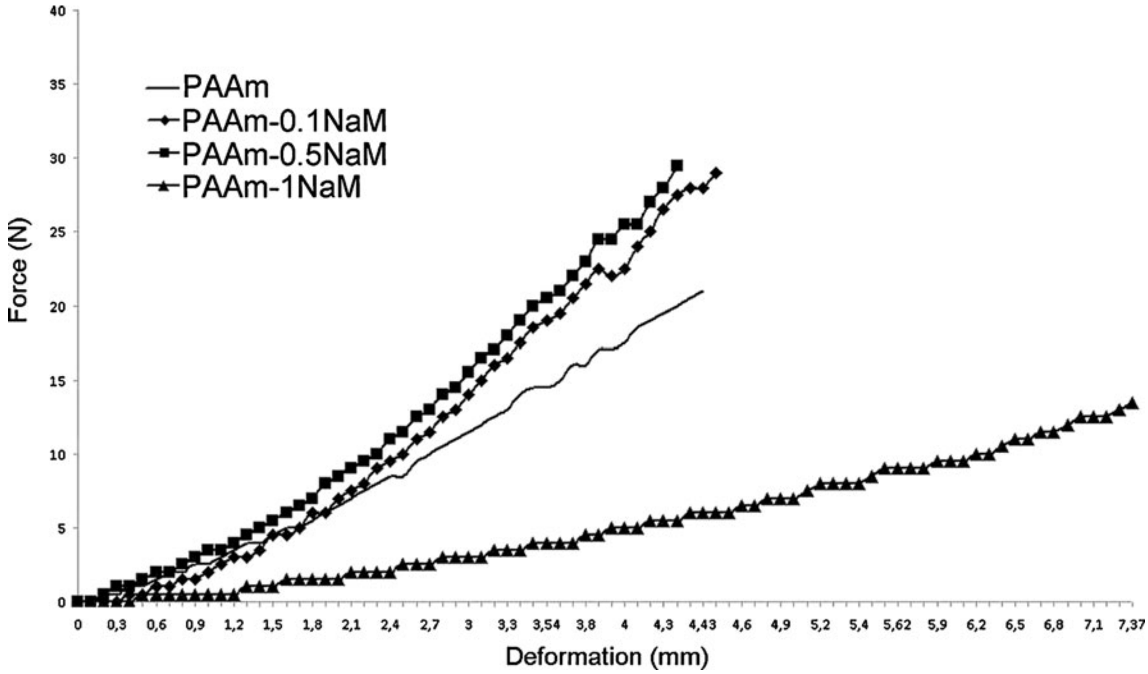

Fig. 10 Force-deformation curves of PAAm and PAAm-NaM hydrogels

the organic crosslinkler, EGDMA. Moreover, this "effective" participation of clay into crosslinking reaction also leads to formation of a stretchable microcomplex structure due to the existence of higher amount of ionic interaction of negatively charged nano-sized clay surface and positively charged quaternary ammonium groups connected to network matrix throughout the covalent bonds. The more viscous character of the nanocomposite hydrogels over conventional OR gels has been already pointed out with some viscoelastic measurements in the literature [21, 26, 27]. It is quite clear that these sites are acting as a kind of reversible physical crosslinking resulting in more viscous character in network. In this study, it is obvious that having very large surface area due to the exfoliated nano-sized platelets in the matrix also gives rise to increase in number of ionic interaction between surface and network matrix by exhibiting more viscous character. The quite low compression resistance of highly loaded PAAM-1OrgM sample may be attributed to the partially exfoliated structure (Fig. 5) with some aggreagate formation leading to less surface area as well as less reversible ionic interaction sides leading to compact and rigid nature. Most probably, abovementioned reversible

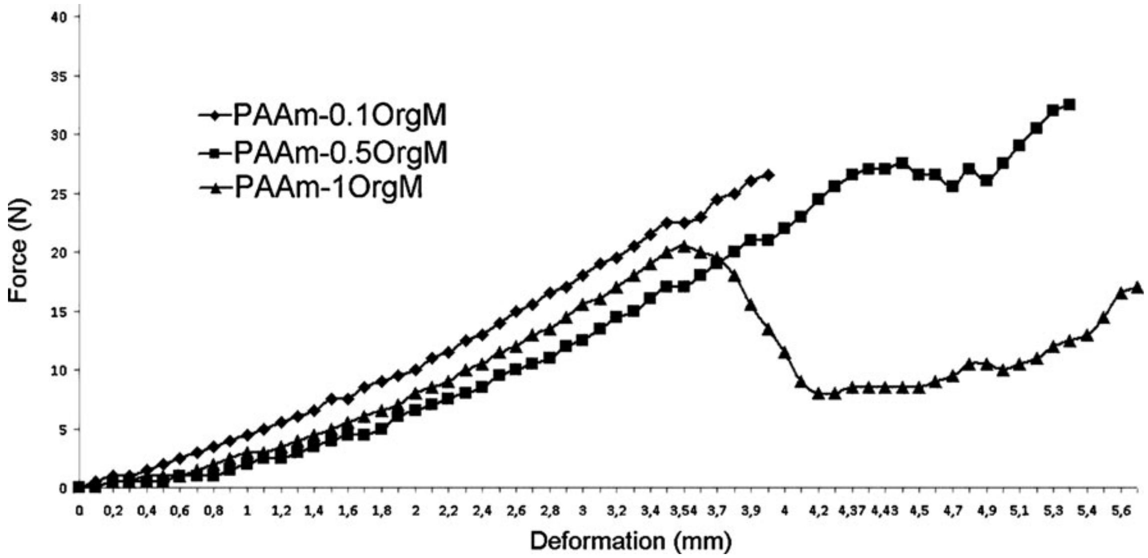

Fig. 11 Force-deformation curves of PAAm-OrgM hydrogels

Table 2 Mechanical properties of PAAm hydrogels

Hydrogels	Elastic Modulus (N mm^{-2})	Max Compression Force (N)	Compression Strength (kPa)
Neat PAAm	0.29	21.00	57.04
PAAm-0.1NaM	0.20	29.00	85.50
PAAm-0.5NaM	0.21	29.50	79.39
PAAm-1NaM	0.37	13.50	37.67
PAAm-0.1OrgM	0.46	26.50	83.76
PAAm-0.5OrgM	0.50	32.50	95.18
PAAm-1OrgM	0.38	20.50	58.96

crosslinked chains may be serving also to high swelling values with a kind of “spongy character”. It is very interesting that the highest swollen-nanocomposite, PAAm-0.5OrgM hydrogel, exhibits much larger elastic modulus and strength compared with other PAAm gels most probably due to both homogeneous and fine dispersion of nano-sized layers forming optimum amount of reversible interconnected subnetwork in matrix network as a powerful morphology.

SEM images in Fig. 12 shows the changes in morphology of the hydrogels in swollen states via nanocomposite formation.

It is quite clear that neat PAAM hydrogel (Fig. 12a) exhibits somewhat porous structure but mostly having closed cells with few *ca* 25–100 μm sized open cells. In the case of unmodified clay additions (Fig. 12b, c, d), number of dispersed and nano-sized clay directed open cell

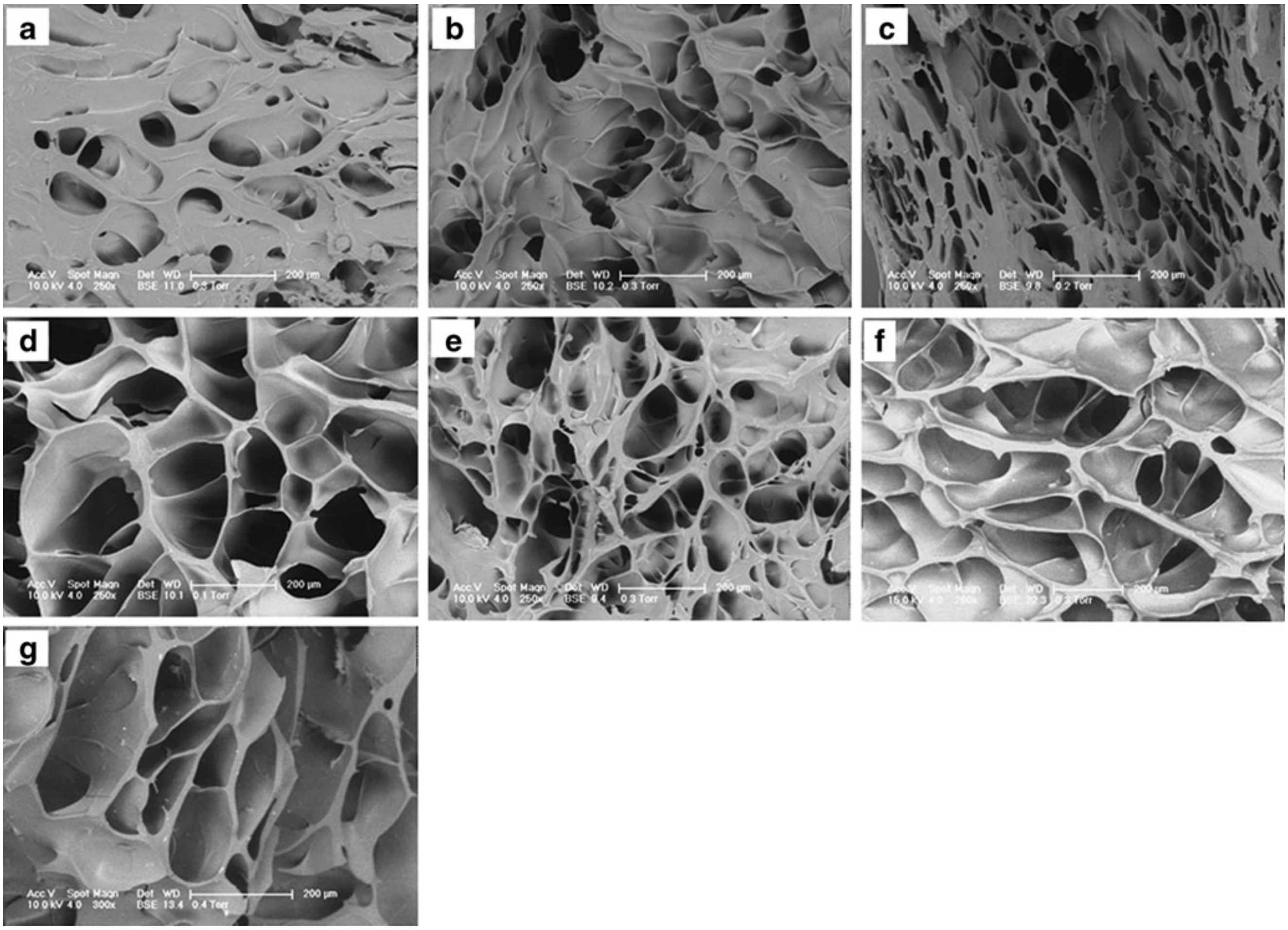

Fig. 12 SEM images of (**a**) PAAm, (**b**) PAAm-0.1NaM, (**c**) PAAm-0.5NaM, (**d**) PAAm-1NaM, (**e**) PAAm-0.1OrgM, (**f**) PAAm-0.5OrgM and (**g**) PAAm-1OrgM hydrogels

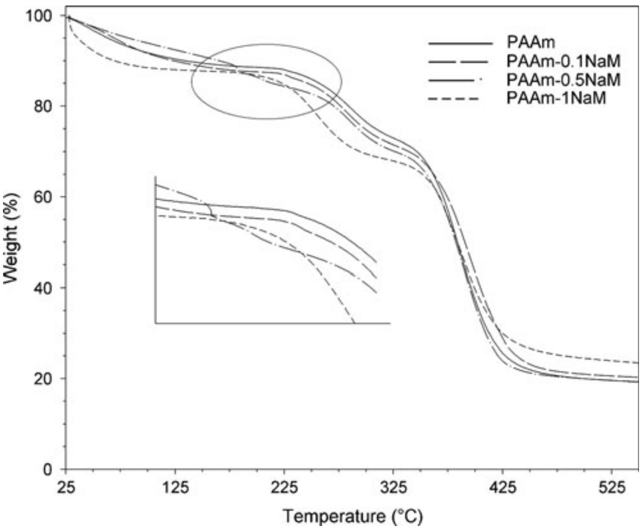

Fig. 13 TGA thermograms of PAAm and PAAm-NaM hydrogels

structures dominate with the still existence of some closed cells. Moreover as clay loading increases, cell size increases from *ca* 100 μm to *ca* 300 μm. Most interestingly, although the organophilic clay in Fig. 12e–g exhibit the similar trend up to 0.5% loading with the highest open cell sizes *ca* 400 μm (Fig. 12f), at 1% loading these sizes show a decrease to *ca* 200 μm (Fig. 12g). The higher sizes in open cells for organophilic clay nanocomposites may be resulted from the formation of sub-networks having extended crosslinking chains by leaving much larger pores behind. Especially in 0.5% OrgMMT loading, this morphology having largest open cells also additionally contains, in one big cell, lots of interconnected rooms (Fig. 12f) which make it more attractive for the solvent accommodation and helping also in sharing the applied compressive forces effectively. This special and beneficial morphology is believed to lead to both maximum swelling as well as compression strength. On the other hand, most probably due to the aggregation resulted intercalation in PAAm-1OrgM (Fig. 4), the lack of the abovementioned interconnected rooms as well as large open cells makes it ineffective in both swelling and mechanical strength.

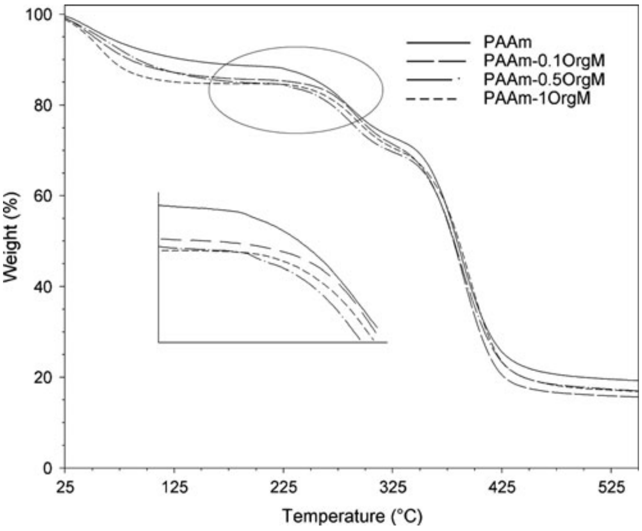

Fig. 14 TGA thermograms of PAAm and PAAm-OrgM hydrogels

The thermal stabilities of the nanocomposite hydrogels were studied by thermogravimetric analysis (TGA). It is clear from the Fig. 13 and Fig. 14 that compared to neat PAAm gel, the onset temperature of degradation was found to be increased by almost 40 °C via adding OrgMMT clay. Higher thermal stability in PAAm-OrgM nanocomposite hydrogels than PAAm-NaM ones might be attributed to extensive interaction between the OrgMMT clay and the polymer resulted from the availability of a larger surface area of OrgMMT clay for the polymer matrix as well as formation of sub-networks, so leading to restricted molecular mobility of the polymer chains and resulting in inhibition of the diffusion of the decomposed product in the polymer matrix [28].

Conclusions

Nanocomposite hydrogels were prapered by *in situ* free radical polymerization of AAm in the presence of the water-swollen inorganic clay with organic crosslinker, EGDMA. Either sodium or organically and functionally modified montmorillonite was used as clay nanoparticles in different loading degrees. The effect of both clay loading and intercalant with double bond contribution on hydrogel properties were discussed in terms of mechanical, swelling and thermal properties. Success in both intercalation of intercalant into MMT clay layers through the ion-exchange reaction and exfoliation in PAAm matrix were confirmed via XRD, TGA and AFM analyses. Swelling studies showed that the maximum attainable swelling in neat PAAm network having crosslinker is 577% whereas the values for most nanocomposite hydrogels are higher. Moreover, insertion of OrgMMT clay into hydrogel at 0.5% loading, on the other hand, causes to a peak in swelling values up to 700%. It was also found that the nanocomposite hydrogel, PAAm-0.5OrgM exhibited the higher sized - open cells with interconnected rooms inside as compared to the other nanocomposite hydrogels which make it more attractive for the solvent accommodation. Also, this highest swollen-nanocomposite hydrogel, exhibits its superior elastic modulus and strength values compared with other PAAm gels due to the optimum amount of reversible interconnected subnetwork in matrix network helping also in sharing the applied compression forces effectively. TG analysis showed that as compared to neat

PAAm gel, in contrast to PAAm-NaM hydrogels, the onset temperature of degradation was found to be increased by almost 40 °C via adding OrgMMT clay.

Finally it can be safely concluded that nanocomposite hydrogels can be tuned for serving as a good water absorber, thermally stable as well as high strength hydrogels by using functionally and organically modified clay in optimum amount around 0.5%.

Acknowledgements Supports given by Bogazici University Research Foundation (projects no. BAP5705), Yalova University Scientific Research Projects Coordination Department (Projects no. 2010–003) and Scientific and Technological Research Council of Turkey (TUBİTAK) (Project no. 110 M029) are gratefully acknowledged.

References

1. Matsumoto A, Yoshida R, Kataoka K (2004) glucose-responsive polymer gel bearing phenylborate derivative as a glucose-sensing moiety operating at the physiological pH. Biomacromolecules 5:1038–1045
2. Stayton PS, Shimoboji T, Long C, Chilkoti A, Chen G, Harris JM, Hoffman AS (1995) Control of protein-ligand recognition using a stimuli-responsive polymer. Nature 378:472–474
3. Orakdogen N, Okay O (2006) Reentrant conformation transition in poly(N, N-dimethylacrylamide) hydrogels in water-organic solvent mixtures. Polymer 47:561–568
4. Byrne ME, Park K, Pepas NA (2002) Molecular imprınting within hydrogels. Adv Drug Delivery Rev 54:149–161
5. Wu YT, Zou Z, Fan QQ (2009) Facile *in-situ* fabrication of novel organic nanoparticle hydrogels with excellent mechanical properties. J Mater Chem 19:7340–7346
6. Lin J, Tang Q, Hu D, Sun X, Li Q, Wu J (2009) Electric field sensitivity of conducting hydrogels with interpenetrating polymer network structure. Colloid Surface A 346:177–183
7. Sun X, Li Q, Wu J, Lin J, Huang M, Tang Q (2009) A simple route to high-strength hydrogel with an interpenetrating polymer network. E-Polymers 90:1–6
8. Lin J, Xu S, Shi X, Feng S, Wang J (2009) Synthesis and properties of a novel double network nanocomposite hydrogel. Polym Adv Technol 20:645–649
9. Li B, Jiang Y, Liu Y, Wu Y, Ren H, Zhu B, Zhu M (2009) Preparation and characterization of inorganic/organic crosslinking poly(*n*-isopropylacrylamide)/poly(acrylamide) interpenetrating network hydrogels. Acta Polym Sin 5:419–424
10. Qin X, Zhao F, Liu Y, Wang H, Feng S (2009) High mechanical strength hydrogels preparation using hydrophilic reactive microgels as crosslinking agents. Colloid Polym Sci 287:621–625
11. Abdurrahmanoglu S, Can V, Okay O (2008) Equilibrium swelling behavior and elastic properties of polymer–clay nanocomposite hydrogels. J Appl Polym Sci 109:3714–3724
12. Li P, Siddaramaiah KNH, Yoo GH, Lee JH (2009) Poly(acrylamide/laponite) nanocomposite hydrogels: Swelling and cationic dye adsorption properties. J Appl Polym Sci 111:1786–1798
13. Okay O, Oppermann W (2007) Polyacrylamide–clay nanocomposite hydrogels: rheological and light scattering characterization. Macromolecules 40:3378–3387
14. Xiong L, Hu X, Liu X, Tong Z (2008) Network chain density and relaxation of *in situ* synthesized polyacrylamide/hectorite clay nanocomposite hydrogels with ultrahigh tensibility. Polymer 49:5064–5071
15. Gao D, Heimann RB, Williams MC, Wardhaugh LT, Muhammad M (1999) Rheological properties of poly(acrylamide)-bentonite composite hydrogels. J Mater Sci 34:1543–1552
16. Zolfaghari R, Katbab AA, Nabavizadeh J, Yousefzade R, Nejad M (2006) Preparation and characterization of nanocomposite hydrogels based on polyacrylamide for enhanced oil recovery applications. J Appl Polym Sci 100:2096–2103
17. Memeşa M, Menceloğlu Y, Nugay T, Nugay N (2004) Layered silica modification with reactive groups for polystyrene nanocomposites. Polym Preprint Am Chem Soc Div Polym Chem 45:806–807
18. Alexandre M, Dubois P (2000) Polymer layered silicate nanocomposites: preparation, properties and uses of a new class of materials. Mater Sci Eng R: Reports 28:1–63
19. Zilg C, Mülhaupt R, Finter J (1999) Morphology and toughness/stiffness balance of nanocomposites based upon anhydride-cured epoxy resins and layered silicates. Macromol Chem Phys 200:661–670
20. Reichert P, Nitz H, Klinke S, Brandsch R, Thomann R, Mülhaupt R (2000) Poly(propylene)/organoclay nanocomposite formation: Influence of compatibilizer functionality and organoclay modification. Macromol Mater Eng 275:8–17
21. Haraguchi K, Takehisa T, Fan S (2002) effects of clay content on the properties of nanocomposite hydrogels composed of poly(*N*-isopropylacrylamide) and clay. Macromolecules 35:10162–10171
22. Haraguchi K (2007) Nanocomposite Hydrogels. Curr Opin Solid State Mater Sci 11:47–54
23. Messersmith PB, Znidarsich F (1997) Synthesis and LCST behavior of thermally responsive poly(N-isopropylacrylamide)/layered silicate nanocomposites. Mat Res Soc Symp 457:507–512
24. Liang L, Liu J, Gong X (2000) Thermosensitive poly(N-isopropylacrylamide)-clay nanocomposites with enhanced temperature response. Langmuir 16:9895–9899
25. Haraguchi K, Song L (2007) Microstructures formed in co-crosslinked networks and their relationships to the optical and mechanical properties of PINA/clay nanocomposite gels. Macromolecules 40:5526–5536
26. Haraguchi K, Li HJ (2006) Mechanical properties and structure of polymer-clay nanocomposite gels with high clay content. Macromolecules 39:1898–1905
27. Haraguchi K, Farnworth R, Ohbayashi A, Takehisa T (2003) Compositional Effects on Mechanical Properties of Nanocomposite Hydrogels Composed of Poly(N,N-Dimethylacrylamide) and Clay. Macromolecules 36:5732–5741
28. Leszczynska A, Njuguna J, Pielichowski K, Banerjee JR (2007) Polymer/montmorillonite nanocomposites with improved thermal properties. Thermochim Acta 453:75–96